Chinese Journal of Chemistry, **2004**, *22*, 1115—1122

Article

Thermokinetic Study on the Complexation Reaction of the First-Row Transitional Metal Chlorides with Histidine

CHEN, San-Ping(陈三平)　　GAO, Sheng-Li*(高胜利)　　SHI, Qi-Zhen(史启祯)

Shaanxi key Laboratory of Physico-inorganic Chemistry, Department of Chemistry, Northwest University, Xi'an, Shaanxi 710069, China

The enthalpy change of the complexation reactions of the first-row transitional metal chlorides including $CrCl_3$, $MnCl_2$, $FeCl_2$, $CoCl_2$, $NiCl_2$ and $CuCl_2$ with *L*-*α*-histidine in water were determined by a microcalorimeter at 298.15—323.15 K. The standard enthalpy of formation of $Cr(His)_2^{3+}$ (aq) and $M(His)_2^{2+}$ (aq) (M＝Mn, Fe, Co, Ni and Cu) were calculated. Based on the thermodynamic and kinetic equations of the reactions, three thermodynamic parameters (the activation enthalpy, the activation entropy, the activation free energy), the rate constants, and three kinetic parameters (the apparent activation energy, the pre-exponential constant and the reaction order) are obtained. The solid complexes of $CrCl_3$, $MnCl_2$, $FeCl_2$, $CoCl_2$, $NiCl_2$ and $CuCl_2$ with histidine were prepared and identified as $Cr(His)_2Cl_3•H_2O$, $Mn(His)_2Cl_2•4H_2O$, $Fe(His)_2Cl_2•H_2O$, $Co(His)_2Cl_2•H_2O$, $Ni(His)_2Cl_2•H_2O$ and $Cu(His)_2Cl_2•H_2O$ by chemical and elemental analyses. The bonding characteristics of these complexes were characterized by IR as well. The results showed that, with the atomic number increasing, three thermodynamic parameters, $\Delta G_{\ominus}^{\neq}$, $\Delta H_{\ominus}^{\neq}$ and $\Delta S_{\ominus}^{\neq}$ of the complexation reaction of these metal chlorides with *L*-*α*-histidine in water present an analogy regularity.

Keywords　first-row transitional metal chloride, *L*-*α*-histidine, complex, formation reaction, thermokinetics

Introduction

The first-row transitional metals of chromium, manganese, iron, cobalt, nickel and copper are essential trace elements to human body, which are connected with hundreds of metalloproteins and metalloenzymes, participating in ferment syntheses and playing an important role in metabolism of nucleic acid, protein, carbohydrate and fat. *L*-*α*-histidine is one of the basic units of proteins and absorbed from food because of not being synthesized in human body. Therefore, it is of practical significance for understanding the complexes of trace elements with *L*-*α*-histidine.

Changes in heat constitute the most essential aspect of chemical processes. The determination of the reaction progress depends on energy changes. Microcalorimeters are therefore used in a broad range of application, for example, ligand binding studies, dissolution and sorption measurements, estimation of the stability of chemical substances and technical products, and measurements of metabolic reactions in cellar systems.[1] Isothermal microcalorimetric techniques have been improved during the past decades, and several types of instruments are commercially available. An RD-496 III type microcalormeter possesses a good performance of high stability, sensitivity, precision and being controlled by computer.[2] The computer program is designed under a window system, which directly displays thermal effect with reaction progress and records the whole thermodynamic curve. So, it suits for the kinetic study of reaction system from a calorimetric investigation.

In this report, the enthalpy changes of the complexation reactions of the first-row transitional metal chlorides including $CrCl_3•6H_2O$, $MnCl_2•4H_2O$, $FeCl_2•4H_2O$, $CoCl_2•2H_2O$, $NiCl_2•6H_2O$ and $CuCl_2•2H_2O$ with *L*-*α*-histidine in water have been determined by a microcalorimeter at 298.15—323.15 K. Fundamental parameters for the title reactions, the reaction rate constant (k), the apparent activation energy (E), the pre-exponential constant (A), the reaction order (n), the activation enthalpy ($\Delta H_{\ominus}^{\neq}$), the activation entropy ($\Delta S_{\ominus}^{\neq}$) and the activation free energy ($\Delta G_{\ominus}^{\neq}$) were abtained on the basis of thermodynamic and kinetic equations of the reactions. Six solid complexes were prepared and identified as $Cr(His)_2Cl_3•H_2O$, $Mn(His)_2Cl_2•4H_2O$, $Fe(His)_2Cl_2•H_2O$, $Co(His)_2Cl_2•H_2O$, $Ni(His)_2Cl_2•H_2O$ and $Cu(His)_2Cl_2•H_2O$, and the bonding characteristics of the complexes were characterized by IR as well.

Experimental

Materials

$CrCl_3•6H_2O$, $MnCl_2•4H_2O$, $FeCl_2•4H_2O$, $CoCl_2•$

* E-mail: gaoshli@nwu.edu.cn.
Received March 8, 2003; revised July 8, 2004; accepted September 1, 2004.
Projected supported by the National Natural Science Foundation of China (Nos. 299871032 and 20171036) and the National Natural Science Foundation of Shaanxi Province (No. FF02328).

$2H_2O$, $NiCl_2$•$6H_2O$ and $CuCl_2$•$2H_2O$ are of A.R. grade, and metal chlorides were noted as A. *L*-*α*-histidine (noted as B) was of B.R. grade with the purity of more than 99.5%. They were dissolved in distilled water. The concentration of solution A and B were 0.1000 mol•L^{-1}, and the molar ratio of two solutions, A to B was 1∶2. The conductivity of deionized water was 5.48×10^{-8} S•cm^{-1}.

Experimental equipment and conditions

The thermokinetic reaction was performed by a microcalorimeter (RD496-III, China, Southwest Institute of Electronic Engineering), which was equipped with two 15 mL vessels.[2] After reaching equilibrium, the spacers between the sample and reference vessels were pushed down simultaneously and the samples were mixed. The microcalorimeter was calibrated by the Joule effect and its sensitivity were (63.994±0.042), (64.308±0.027), (64.499±0.064), (64.638±0.078), (64.733±0.077) and (64.739±0.059) μV•mW^{-1} at the experimental temperature of (298.15 ± 0.005) K, (303.15±0.005), (308.15±0.005), (313.15±0.005), (318.15±0.005) and (323.15±0.005) K, respectively. The experimental precision and accuracy were checked by measuring the enthalpy of special purity crystalline KCl in deionized water at 298.15 K. The experimental value of $\Delta_{sol}H_m^\ominus$ is (17.238±0.048) kJ•mol^{-1}, which is in good agreement with that of $\Delta_{sol}H_m^\ominus$ of (17.241 ±0.018) kJ•mol^{-1} reported in the literature.[3] It indicated that the device used in this work was reliable and the precision measured was 0.5%.

Cr^{3+} was determined with ammonium ferrous sulfate, Mn^{2+} was determined by oxidation-reduction with ammonium peroxydisulfate, Fe^{2+} was determined by potassium dichromate method, Co^{2+} and Ni^{2+} were determined complexometrically with EDTA, Cu^{2+} was determined by iodimetry and Cl^- was determined by Fajans' method. Elemental analyses (C, H, and N) were carried out on a 2400-type elemental analyzer of P. E. company. IR spectra for the title complexes were performed with a Model EQ UNINOX-550 FT-IR spectrophotometer (KBr pellet) (Bruker of USA).

Results

The following Eqs. could represent the reaction of solution of metal chlorides with solution of histidine:

$$Cr^{3+}(aq)+2His(aq)\xrightarrow{\Delta H_m^\ominus(1)}Cr(His)_2^{3+}(aq) \quad (1)$$

$$M^{2+}(aq)+2His(aq)\xrightarrow{\Delta H_m^\ominus(2)}M(His)_2^{2+}(aq) \quad (2)$$

(M=Mn, Fe, Co, Ni and Cu)

After calorimetric experiments, the final solutions collected from six experiments for each reaction system were concentrated over P_4O_{10} at the temperature of 298.15 K. The residuals were characterized by chemical and elemental analyses, indicating that they fit into the compositions of $Cr(His)_2Cl_3$•H_2O, $Mn(His)_2Cl_2$•$4H_2O$, $Fe(His)_2Cl_2$•H_2O, $Co(His)_2Cl_2$•H_2O, $Ni(His)_2Cl_2$•H_2O and $Cu(His)_2Cl_2$•H_2O, respectively. The analytical results are listed in Table 1.

IR spectra for the complexes show that characteristic absorption peaks of amino and carboxyl groups have great shifts as compared with those in the free ligand.[4] It indicates that nitrogen and oxygen atoms in the complexes coordinate to M^{n+} in a bidentate fashion. In addition, characteristic absorption peak of imidazolyl group shifts intensively, which shows that nitrogen atom in the imidazolyl group coordinates to M^{n+} as well. The peaks close to 3410 and 828 cm^{-1} of these complexes are assigned to the hydroxy group absorption of water that is present in the complexes.

Combining the elemental analyses with IR spectra for the complexes, it indicates that the formation reactions of the complexes are non-reversible.

Determination of $\Delta_r H_m^\ominus$

Within the range of the experimental temperature, the complxation reactions are exothermic. For each reaction system, $\Delta_r H_m^\ominus$ was measured six times at 298.15 K. The thermodynamic curve of the reaction of copper chloride with *L*-*α*-Histidine thermodynamic curve is shown in Figure 1. $\Delta_r H_m^\ominus$, mean value of six parallel experiments for each reaction system, is listed in Table 2.

Calculation of $\Delta_f H_m^\ominus[M(His)_2^{n+}]$ of hydrate complex cations

Following Eqs. (1) and (2), the standard enthalpies of formation of $M(His)_2^{2+}$ (aq) and $Cr(His)_2^{3+}$ (aq)

Table 1 Analytical results of chemical composition of solid complexes[a]

Complex	M^{n+} /%	Cl^- /%	C/%	H/%	N/%
$Cr(His)_2Cl_3$•H_2O	10.77 (10.69)	21.89 (21.85)	29.68 (29.62)	4.19 (4.14)	17.26 (17.27)
$Mn(His)_2Cl_2$•$4H_2O$	10.79 (10.81)	13.99 (13.95)	28.39 (28.36)	5.21 (5.16)	16.51 (16.54)
$Fe(His)_2Cl_2$•H_2O	13.73 (13.68)	6.01 (5.88)	17.70 (17.65)	2.84 (2.72)	10.31 (10.29)
$Co(His)_2Cl_2$•H_2O	12.90 (12.86)	15.51 (15.48)	31.53 (31.46)	4.47 (4.40)	18.28 (18.34)
$Ni(His)_2Cl_2$•H_2O	12.81 (12.82)	15.52 (15.48)	31.52 (31.48)	4.43 (4.40)	18.33 (18.35)
$Cu(His)_2Cl_2$•H_2O	13.69 (13.73)	15.37 (15.32)	31.17 (31.14)	4.39 (4.36)	18.12 (18.16)

[a] The data in brackets are calculated values.

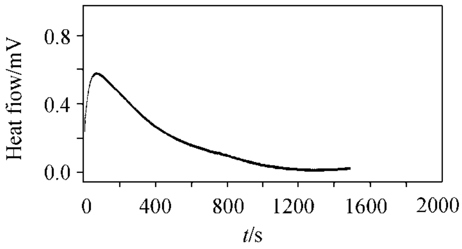

Figure 1 Thermokinetic curve of the reaction $CuCl_2$ with *L*-*α*-histidine at 298.15 K.

is calculated by Hess'law

$$\Delta_f H_m^\ominus[\mathrm{Cr(His)}_2^{n+}, \mathrm{aq}] = \Delta_r H_m^\ominus(1) + \Delta_f H_m^\ominus(\mathrm{Cr}^{3+}) + 2\Delta_f H_m^\ominus(\mathrm{His, aq}) \quad (3)$$

$$\Delta_f H_m^\ominus[\mathrm{M(His)}_2^{2+}, \mathrm{aq}] = \Delta_r H_m^\ominus(2) + \Delta_f H_m^\ominus(\mathrm{M}^{2+}) + 2\Delta_f H_m^\ominus(\mathrm{His, aq}) \quad (4)$$

So, according to the Refs. 5—8, $\Delta_f H_m^\ominus[\mathrm{M(His)}_2^{n+}, \mathrm{aq}]$ of hydrate complex cations are calculated as (−2856.18±3.58), (−1070.19±3.08), (−948.45±3.08), (−920.81±3.08), (−924.03±3.08) and (−818.03±3.19) kJ•mol^{-1} in the sequence of increasing atomic number.

Thermokinetic calculation of the formation reactions of the complex-cations

The original data obtained from the *TK* curve are summarized in Tables 3—8. Referred to reaction thermodynamic and kinetic Eqs. (5)—(8),[9] the reaction rate constant (*k*), the activation energy (*E*), the pre-exponential constant (*A*), the reaction order (*n*), the activation enthalpy ($\Delta H_\ominus^\neq$), the activation entropy ($\Delta S_\ominus^\neq$) and the activation free energy ($\Delta G_\ominus^\neq$) were attained, which are listed in Tables 9—14.

$$\ln\left(\frac{1}{H_0}\frac{\mathrm{d}H_i}{\mathrm{d}t}\right) = \ln k + n\ln\left(1 - \frac{H_i}{H_0}\right) \quad (5)$$

$$\ln k = \ln A - \frac{E}{RT} \quad (6)$$

$$\Delta G_\ominus^\neq = RT\ln\frac{RT}{Nhk} \quad (7)$$

$$\ln\frac{k}{T} = \ln\frac{k_B}{h} + \frac{\Delta S_\ominus^\neq}{RT} - \frac{\Delta H_\ominus^\neq}{RT} \quad (8)$$

Table 2 Enthalpies of 1∶2 liquid-liquid reactions at 298.15 K

Reaction system	$-Q_p$/mJ						−mean/mJ	$-\Delta_r H_m^\ominus$/(kJ•mol^{-1})
$CrCl_3$-His	1460.328	1455.973	1451.618	1450.123	1448.715	1442.908	1451.611±6.022	7.258±0.03
$MnCl_2$-His	36.454	36.302	36.219	36.363	36.146	36.002	36.248±0.161	0.121±0.06
$FeCl_2$-His	2879.869	2860.438	2859.850	2856.120	2854.130	2842.691	2859.850±12.532	9.533±0.04
$CoCl_2$-His	3862.406	3847.064	3835.557	3829.031	3827.886	3812.544	3835.74±17.229	12.786±0.06
$NiCl_2$-His	6105.896	6084.674	6063.452	6058.338	6021.009	6063.610	6063.610±29.357	20.212±0.09
$CuCl_2$-His	10245.119	10194.274	10168.853	10146.223	10148.515	10107.840	10168.470±21.081	33.895±0.157

Table 3 Thermographic data of reaction of $CrCl_3$•$6H_2O$ with *L*-*α*-His [a]

t/s	298.15 K		303.15 K		308.15 K		313.15 K		318.15 K		323.15 K	
	H_i/H_0	dH_i/d*t* 10^4/(J•s^{-1})	H_i/H_0	dH_i/d*t* 10^4/(J•s^{-1})	H_i/H_0	dH_i/d*t* 10^4/(J•s^{-1})	H_i/H_0	dH_i/d*t* 10^4/(J•s^{-1})	H_i/H_0	dH_i/d*t* 10^4/(J•s^{-1})	H_i/H_0	dH_i/d*t* 10^4/(J•s^{-1})
100											0.2197	4.47
150											0.3522	9.65
200									0.4059	43.35	0.4791	1.86
250							0.3635	29.94	0.4926	36.92	0.5970	36.96
300			0.1527	17.69	0.4462	16.08	0.5065	24.36	0.5800	31.25	0.7179	27.20
350	0.1617	10.69	0.1897	16.89	0.5837	11.99	0.6078	20.14	0.6318	26.48	0.8172	17.37
400	0.2005	10.18	0.2198	16.51	0.6877	9.877	0.6800	16.81	0.6871	22.42	0.8865	11.47
450	0.2321	9.942	0.2421	15.99	0.7608	7.454	0.7329	14.30	0.7347	19.10	0.9224	7.989
500	0.2554	9.613	0.2671	15.53	0.8116	5.924	0.7727	12.22	0.7758	16.36	0.9479	4.072
550	0.9346	9.321	0.2860	14.88	0.8432	4.959	0.8033	10.33	0.8113	13.98	0.9613	4.072
600	0.3012	8.906	0.3124	14.49	0.8683	4.369	0.8274	8.928	0.8419	11.98		
650	0.3286	8.664	0.3388	14.03	0.8867	3.538	0.8464	7.762	0.8681	10.20		
700	0.3561	8.371	0.3652	13.46	0.9038	2.994	0.8615	6.949				
750	0.3833	8.014	0.4048	12.82	0.9215	2.563						
800	0.4237	7.608										

[a] H_0=1.239 (298.15 K), 1.416 (303.15 K), 1.517 (308.15 K), 2.085 (313.15 K), 2.299 (318.15 K) and 2.537 J (323.15 K).

Table 4 Thermographic data of reaction of $MnCl_2•4H_2O$ with *L*-*α*-His [a]

t/s	298.15 K		303.15 K		308.15 K		313.15 K		318.15 K		323.15 K	
	H_i/H_0	dH_i/dt $10^4/(J•s^{-1})$	H_i/H_0	dH_i/dt $10^4/(J•s^{-1})$	H_i/H_0	dH_i/dt $10^4/(J•s^{-1})$	H_i/H_0	dH_i/dt $10^4/(J•s^{-1})$	H_i/H_0	dH_i/dt $10^4/(J•s^{-1})$	H_i/H_0	dH_i/dt $10^4/(J•s^{-1})$
70	0.3184	4.232	0.2304	8.185	0.2655	11.48	0.2256	14.34	0.2290	19.19	0.1674	23.10
90	0.4073	4.017	0.3105	7.893	0.3466	10.96	0.2997	13.89	0.3013	18.47	0.2501	22.41
110	0.4871	3.747	0.3859	7.507	0.4211	10.34	0.3695	13.27	0.3696	17.57	0.3148	21.02
130	0.5578	3.488	0.4555	7.051	0.4888	9.705	0.4344	12.58	0.4335	16.59	0.3778	19.64
150	0.6200	3.224	0.5194	6.601	0.5499	9.075	0.4945	11.83	0.4928	15.73	0.4556	18.50
170	0.6744	2.981	0.5776	6.179	0.6049	8.489	0.5497	11.13	0.4524	14.75	0.5129	17.65
190	0.7220	2.739	0.6306	5.769	0.6541	7.919	0.6001	10.48	0.5981	13.89	0.5685	16.78
210	0.7633	2.522	0.6785	5.361	0.6983	7.380	0.6461	9.856	0.6445	13.07	0.6129	15.66
230	0.7993	2.320	0.7217	4.974	0.7376	6.886	0.6880	9.179	0.6868	12.26	0.6690	14.54
250	0.8304	2.219	0.7606	4.643	0.7724	6.423	0.7259	8.622	0.7253	11.52	0.7193	13.33

[a] H_0=0.142 (298.15 K), 0.226 (303.15 K), 0.282 (308.15 K), 0.306 (313.15 K), 0.356 (318.15 K) and 0.362 J (323.15 K).

Table 5 Thermographic data of reaction of $FeCl_2•4H_2O$ with *L*-*α*-His [a]

t/s	298.15 K		303.15 K		308.15 K		313.15 K		318.15 K		323.15 K	
	H_i/H_0	dH_i/dt $10^4/(J•s^{-1})$	H_i/H_0	dH_i/dt $10^4/(J•s^{-1})$	H_i/H_0	dH_i/dt $10^4/(J•s^{-1})$	H_i/H_0	dH_i/dt $10^4/(J•s^{-1})$	H_i/H_0	dH_i/dt $10^4/(J•s^{-1})$	H_i/H_0	dH_i/dt $10^4/(J•s^{-1})$
200	0.3599	18.52	0.3982	24.69	0.3889	36.12	0.3916	44.67	0.4687	55.44	0.4053	72.50
300	0.5027	15.88	0.5482	19.50	0.5242	27.27	0.5222	34.84	0.6090	42.56	0.5535	56.69
400	0.5943	12.59	0.6477	14.77	0.6229	20.88	0.6154	27.54	0.7024	32.76	0.6494	44.73
500	0.6929	8.905	0.7208	11.44	0.6966	16.33	0.6840	22.29	0.7662	25.50	0.7180	35.68
600	0.7585	6.931	0.7759	9.099	0.7529	13.11	0.7358	18.38	0.8108	20.21	0.7534	28.71
700	0.8111	5.497	0.8183	7.379	0.7970	10.72	0.7759	15.45	0.8432	16.39	0.8055	23.84
800	0.8621	4.393	0.8518	6.315	0.8322	8.972	0.8077	13.31	0.8677	13.88	0.8345	20.10
900	0.8868	3.625	0.8787	5.285	0.8609	7.773	0.8338	11.83	0.8870	12.03	0.8572	17.27
1000	0.9136	2.699	0.9010	4.562	0.8849	6.748	0.8559	10.74	0.9026	10.56	0.8758	15.37
1100	0.9346	2.255	0.9171	3.505	0.9048	5.953	0.8747	9.898	0.9154	9.512	0.8916	13.87

[a] H_0=2.066 (298.15 K), 2.282 (303.15 K), 2.427(308.15 K), 2.474 (313.15 K), 2.972 (318.15 K) and 2.860 J (323.15 K).

Table 6 Thermographic data of reaction of $CoCl_2•2H_2O$ with *L*-*α*-His[10] [a]

t/s	298.15 K		303.15 K		308.15 K		313.15 K		318.15 K		323.15 K	
	H_i/H_0	dH_i/dt $10^4/(J•s^{-1})$	H_i/H_0	dH_i/dt $10^4/(J•s^{-1})$	H_i/H_0	dH_i/dt $10^4/(J•s^{-1})$	H_i/H_0	dH_i/dt $10^4/(J•s^{-1})$	H_i/H_0	dH_i/dt $10^4/(J•s^{-1})$	H_i/H_0	dH_i/dt $10^4/(J•s^{-1})$
200	0.4053	22.39	0.4172	31.53	0.3929	42.69	0.4109	52.91	0.4085	72.09	0.3467	107.1
250	0.4897	19.37	0.5027	26.72	0.4742	37.16	0.4905	46.07	0.4851	62.16	0.4227	96.64
300	0.5636	16.61	0.5769	22.50	0.5452	32.18	0.5592	40.01	0.5516	53.60	0.4921	84.63
350	0.6278	14.20	0.6410	18.92	0.6069	27.84	0.6186	34.71	0.6095	46.31	0.5539	74.00
400	0.6835	12.08	0.6963	15.96	0.6605	24.09	0.6698	30.10	0.6599	40.17	0.6096	64.65
450	0.7314	10.26	0.7440	13.49	0.7070	20.85	0.7138	26.11	0.7041	34.79	0.6579	56.41
500	0.7726	8.729	0.7851	11.41	0.7473	18.07	0.7518	22.68	0.7428	30.33	0.7012	49.33
550	0.8080	7.428	0.8205	9.674	0.7822	15.63	0.7845	19.70	0.7770	26.55	0.7397	43.32
600	0.8384	6.348	0.8509	8.239	0.8123	13.62	0.8218	17.18	0.8074	23.25	0.7740	36.10
650	0.8646	5.471	0.8770	7.052	0.8385	11.94	0.8372	14.97	0.8344	20.39	0.8043	33.49

[a] H_0=3.211 (298.15 K), 3.520 (303.15 K), 3.590 (308.15 K), 3.619 (313.15 K), 3.836 (318.15 K) and 4.066 J (323.15 K).

Table 7 Thermographic data of reaction of $NiCl_2 \cdot 6H_2O$ with *L*-*α*-His [a]

t/s	298.15 K		303.15 K		308.15 K		313.15 K		318.15 K		323.15 K	
	H_i/H_0	dH_i/dt $10^4/(J \cdot s^{-1})$	H_i/H_0	dH_i/dt $10^4/(J \cdot s^{-1})$	H_i/H_0	dH_i/dt $10^4/(J \cdot s^{-1})$	H_i/H_0	dH_i/dt $10^4/(J \cdot s^{-1})$	H_i/H_0	dH_i/dt $10^4/(J \cdot s^{-1})$	H_i/H_0	dH_i/dt $10^4/(J \cdot s^{-1})$
200	0.3977	64.16	0.3635	79.00	0.3796	108.7	0.4339	124.2	0.4435	151.5	0.4127	199.0
250	0.4788	55.78	0.4367	72.98	0.4560	94.71	0.5176	106.6	0.5272	129.5	0.4923	170.7
300	0.5499	48.43	0.5007	67.33	0.5228	82.85	0.5891	91.38	0.5984	110.3	0.5616	146.5
350	0.6121	41.86	0.5564	59.88	.0.5816	72.77	0.6502	78.34	0.6589	93.99	0.6220	125.9
400	0.6663	36.06	0.6051	53.27	0.6334	64.17	0.7024	67.16	0.7103	80.26	0.6744	108.1
450	0.7135	31.09	0.6477	47.35	0.6793	56.48	0.7470	57.36	0.7541	68.33	0.7201	92.86
500	0.7546	26.72	0.6851	42.51	0.7198	49.69	0.7850	49.02	0.7913	58.17	0.7599	79.95
550	0.7902	22.90	0.7182	38.82	0.7554	43.63	0.8174	41.84	0.8229	49.53	0.7945	68.67
600	0.8260	19.62	0.7474	33.50	0.7869	38.26	0.8449	35.78	0.8498	42.12	0.8247	58.95
650	0.8477	16.78	0.7735	29.29	0.8146	33.71	0.8711	29.84	0.8726	35.83	0.8508	50.60

[a] H_0=5.489 (298.15 K), 5.500 (303.15 K), 5.657 (308.15 K), 5.874 (313.15 K), 5.920 (318.15 K) and 6.056 J (323.15 K).

Table 8 Thermographic data of reaction of $CuCl_2 \cdot 2H_2O$ with *L*-*α*-His [a]

t/s	298.15 K		303.15 K		308.15 K		313.15 K		318.15 K		323.15 K	
	H_i/H_0	dH_i/dt $10^4/(J \cdot s^{-1})$	H_i/H_0	dH_i/dt $10^4/(J \cdot s^{-1})$	H_i/H_0	dH_i/dt $10^4/(J \cdot s^{-1})$	H_i/H_0	dH_i/dt $10^4/(J \cdot s^{-1})$	H_i/H_0	dH_i/dt $10^4/(J \cdot s^{-1})$	H_i/H_0	dH_i/dt $10^4/(J \cdot s^{-1})$
200	0.3857	117.7	0.4291	143.7	0.4077	183.1	0.4170	243.0	0.4025	309.4	0.4266	376.3
250	0.4756	104.3	0.5197	124.3	0.4970	159.9	0.5064	208.8	0.4904	269.4	0.5094	323.1
300	0.5553	90.96	0.5978	105.7	0.5750	137.7	0.5844	178.1	0.5672	231.0	0.5808	276.4
350	0.6247	78.13	0.6642	89.07	0.6424	117.5	0.6492	150.8	0.6336	196.3	0.6424	235.5
400	0.6844	66.40	0.7204	74.76	0.7001	99.40	0.7051	127.2	0.6905	166.1	0.6952	200.7
450	0.7354	56.02	0.7678	62.45	0.7492	83.62	0.7524	107.0	0.7391	140.1	0.7404	171.2
500	0.7786	46.90	0.8075	52.09	0.7906	70.00	0.7925	90.05	0.7806	118.1	0.7791	145.9
550	0.8151	39.16	0.8408	43.41	0.8256	58.45	0.8263	75.87	0.8160	99.28	0.8123	124.4
600	0.8457	32.68	0.8687	36.24	0.8551	48.72	0.8550	63.84	0.8460	83.23	0.8406	106.2
650	0.8715	27.20	0.8920	30.26	0.8799	40.55	0.8792	53.72	0.8716	69.82	0.8648	90.69

[a] H_0=8.836 (298.15 K), 9.414 (303.15 K), 9.489 (308.15 K), 10.169 (313.15 K), 10.386 (318.15 K) and 10.497 J (323.15 K).

Table 9 Values of n, k, A, E, $\Delta G_{\ominus}^{\neq}$, $\Delta H_{\ominus}^{\neq}$ and $\Delta S_{\ominus}^{\neq}$ of the reaction of $CrCl_3 \cdot 6H_2O$ with *L*-*α*-His

	Eq. (5)			Eq. (6)			Eq. (6)	Eq. (8)		
T/K	$k\times10^3/s^{-1}$	n	r^a	$E/(kJ \cdot mol^{-1})$	$\ln A$ (A in s^{-1})	r^a	$\Delta G_{\ominus}^{\neq}/(kJ \cdot mol^{-1})$	$\Delta H_{\ominus}^{\neq}/(kJ \cdot mol^{-1})$	$\Delta S_{\ominus}^{\neq}/(J \cdot mol^{-1} \cdot K^{-1})$	r^a
298.15	1.105	0.926	0.998	42.07	10.12	0.998	90.11	34.49	−169.4	0.998
303.15	1.458	0.933	0.998				90.75			
308.15	1.882	0.947	0.999				91.64			
313.15	2.335	0.962	0.997				92.60			
318.15	3.077	0.969	0.999				93.39			
323.15	3.893	0.978	0.998				94.27			

[a] r is the linear correlation coefficient.

Table 10 Values of n, k, A, E, $\Delta G^{\neq}_{\ominus}$, $\Delta H^{\neq}_{\ominus}$ and $\Delta S^{\neq}_{\ominus}$ of the reaction of $MnCl_2 \cdot 4H_2O$ with *L*-*α*-His

	Eq. (5)			Eq. (6)			Eq. (6)	Eq. (8)		
T/K	$k \times 10^3$/s^{-1}	n	r^a	E/(kJ•mol^{-1})	ln A (A in s^{-1})	r^a	$\Delta G^{\neq}_{\ominus}$/(kJ•mol^{-1})	$\Delta H^{\neq}_{\ominus}$/(kJ•mol^{-1})	$\Delta S^{\neq}_{\ominus}$/(J•mol^{-1}•K^{-1})	r^a
298.15	3.680	0.502	0.999	20.68	2.733	0.999	86.92	17.95	−265.0	0.997
303.15	4.201	0.500	0.999				88.08			
308.15	4.798	0.504	0.999				89.24			
313.15	5.416	0.503	0.999				90.41			
318.15	6.189	0.505	0.999				91.55			
323.15	7.026	0.509	0.998				92.69			

^{a} r is the linear correlation coefficient.

Table 11 Values of n, k, A, E, $\Delta G^{\neq}_{\ominus}$, $\Delta H^{\neq}_{\ominus}$ and $\Delta S^{\neq}_{\ominus}$ of the reaction of $FeCl_2 \cdot 4H_2O$ with *L*-*α*-His

	Eq. (5)			Eq. (6)			Eq. (6)	Eq. (8)		
T/K	$k \times 10^3$/s^{-1}	n	r^a	E/(kJ•mol^{-1})	ln A (A in s^{-1})	r^a	$\Delta G^{\neq}_{\ominus}$/(kJ•mol^{-1})	$\Delta H^{\neq}_{\ominus}$/(kJ•mol^{-1})	$\Delta S^{\neq}_{\ominus}$/(J•mol^{-1}•K^{-1})	r^a
298.15	1.388	0.989	0.999	36.77	8.250	0.999	89.34	34.18	−185.0	0.999
303.15	1.775	0.985	0.998				90.26			
308.15	2.257	0.983	0.996				91.17			
313.15	2.838	0.981	0.997				92.10			
318.15	3.565	0.991	0.999				93.00			
323.15	4.342	1.003	0.999				93.98			

^{a} r is the linear correlation coefficient.

Table 12 Values of n, k, A, E, $\Delta G^{\neq}_{\ominus}$, $\Delta H^{\neq}_{\ominus}$ and $\Delta S^{\neq}_{\ominus}$ of the reaction of $CoCl_2 \cdot 2H_2O$ with *L*-*α*-His

	Eq. (5)			Eq. (6)			Eq. (6)	Eq. (8)		
T/K	$k \times 10^3$/s^{-1}	n	r^a	E/(kJ•mol^{-1})	ln A (A in s^{-1})	r^a	$\Delta G^{\neq}_{\ominus}$/(kJ•mol^{-1})	$\Delta H^{\neq}_{\ominus}$/(kJ•mol^{-1})	$\Delta S^{\neq}_{\ominus}$/(J•mol^{-1}•K^{-1})	r^a
298.15	1.145	0.964	0.999	40.17	9.424	0.999	89.81	37.60	−175.2	0.999
303.15	1.471	0.970	0.999				90.73			
308.15	1.921	0.970	0.999				91.58			
313.15	2.472	0.984	0.999				92.46			
318.15	3.112	0.997	0.999				93.36			
323.15	4.016	0.981	0.999				94.19			

^{a} r is the linear correlation coefficient.

Table 13 Values of n, k, A, E, $\Delta G^{\neq}_{\ominus}$, $\Delta H^{\neq}_{\ominus}$ and $\Delta S^{\neq}_{\ominus}$ of the reaction of $NiCl_2 \cdot 6H_2O$ with *L*-*α*-His

	Eq. (5)			Eq. (6)			Eq. (6)	Eq. (8)		
T/K	$k \times 10^3$/s^{-1}	n	r^a	E/(kJ•mol^{-1})	ln A (A in s^{-1})	r^a	$\Delta G^{\neq}_{\ominus}$/(kJ•mol^{-1})	$\Delta H^{\neq}_{\ominus}$/(kJ•mol^{-1})	$\Delta S^{\neq}_{\ominus}$/(J•mol^{-1}•K^{-1})	r^a
298.15	1.921	0.977	0.999	34.31	7.573	0.999	88.53	31.73	−190.6	0.999
303.15	2.331	0.965	0.997				89.57			
308.15	3.009	0.966	0.999				90.43			
313.15	3.703	0.973	0.999				91.40			
318.15	4.549	0.978	0.999				92.36			
323.15	5.518	0.999	0.999				93.33			

^{a} r is the linear correlation coefficient.

Table 14 The values of n, k, A, E, $\Delta G^{\neq}_{\ominus}$, $\Delta H^{\neq}_{\ominus}$ and $\Delta S^{\neq}_{\ominus}$ of the reaction of $CuCl_2$ with L-α-His

	Eq. (5)			Eq. (6)			Eq. (6)	Eq. (8)		
T/K	$k\times10^3/s^{-1}$	n	r^a	$E/(kJ\cdot mol^{-1})$	ln A (A in s^{-1})	r^a	$\Delta G^{\neq}_{\ominus}/(kJ\cdot mol^{-1})$	$\Delta H^{\neq}_{\ominus}/(kJ\cdot mol^{-1})$	$\Delta S^{\neq}_{\ominus}/(J\cdot mol^{-1}\cdot K^{-1})$	r^a
298.15	2.192	0.946	0.999	33.61	7.408	0.999	88.20	31.03	−192.0	0.999
303.15	2.635	0.946	0.999				89.26			
308.15	3.255	0.952	0.999				90.23			
313.15	4.058	0.966	0.999				91.16			
318.15	5.002	0.977	0.999				92.11			
323.15	6.203	0.988	0.999				93.02			

[a] r is the linear correlation coefficient.

Discussions

(1) The experimental results indicate that the title reactions are exothermic and the heat change of the reaction system of $MnCl_2\cdot4H_2O$-His is the least, which is reflected in Figure 2. Furthermore, heat effect for each reaction system increases with increasing temperature. The dependence of heat effect of reaction on temperature is shown in Figure 3.

(2) It is seen from the Tables 3—8 that all the reactions systems are of the first order except that the system of $MnCl_2\cdot4H_2O$-His is of the 0.5 order, which may be attributed to the least heat change. The correlation between reaction rate k and reaction temperature T is depicted in Figure 4, which shows that all the reaction rates increase as the reaction temperature increases. From Figure 5, plots of the activation energies against atomic number, the activation energies of the formation reactions of hydrates of complex cations are far less than 63 $kJ\cdot mol^{-1}$ at which the reaction occurs instantaneously at room temperature. It is thus showed that the title reactions easily occur at 298.15—323.15 K, which is contributed to strong coordination force of histidine.

(3) The variation of thermodynamic functions of $\Delta G^{\neq}_{\ominus}$, $\Delta H^{\neq}_{\ominus}$ and $\Delta S^{\neq}_{\ominus}$ with atomic number are presented in Figures 6, 7 and 8, which are similar to with each other in shape, illuminating that a certain intrinsic regularity is present.

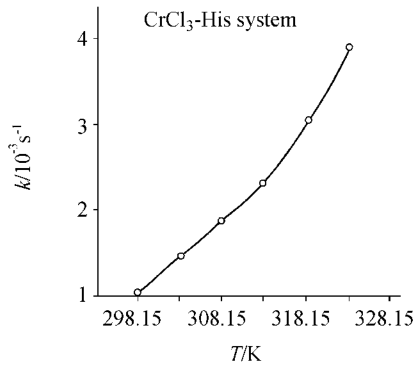

Figure 3 Plots of Q_p against T.

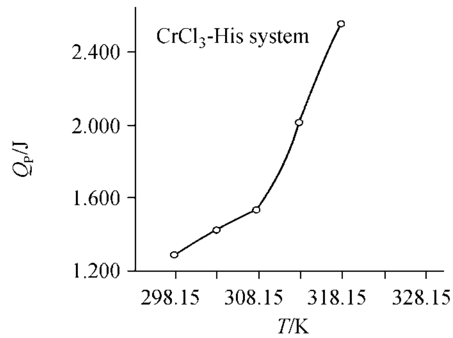

Figure 4 The correlation of reaction rate k and reaction temperature T for $CrCl_3\cdot6H_2O$-His system.

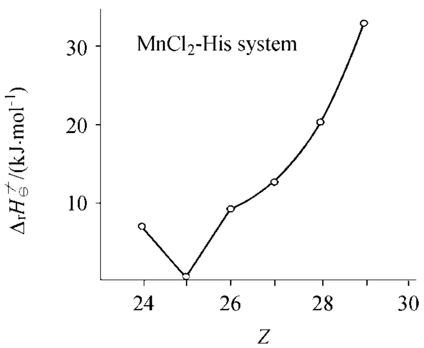

Figure 2 Plots of $\Delta_r H^{\ominus}_m$ against Z.

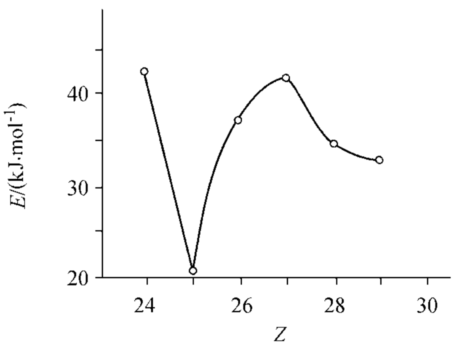

Figure 5 Plots of E against Z.

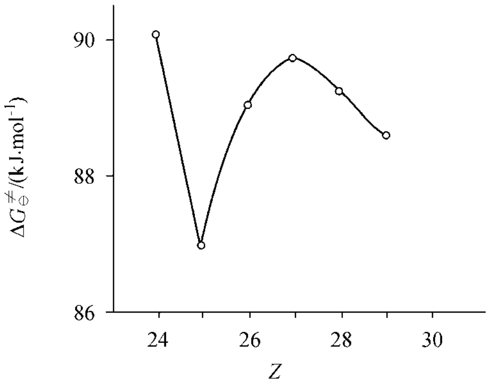

Figure 6 The variation of $\Delta G^{\neq}_{\ominus}$ with *Z*.

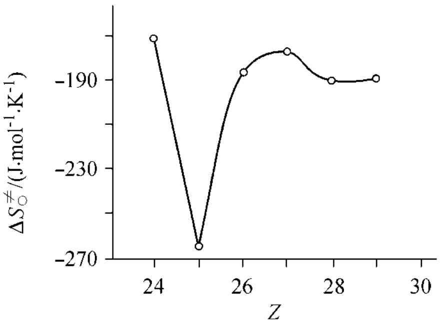

Figure 7 The variation of $\Delta S^{\neq}_{\ominus}$ with *Z*.

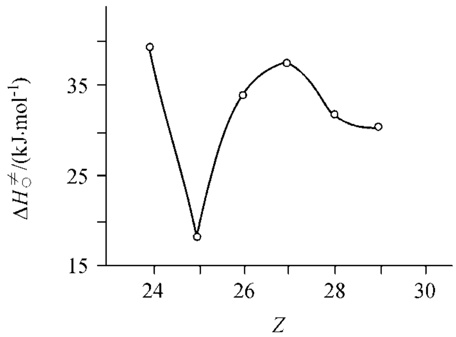

Figure 8 The variation of $\Delta H^{\neq}_{\ominus}$ with *Z*.

Conclusion

The enthalpy changes of the complexation reaction of the first-row transitional metal chlorides including $CrCl_3•6H_2O$, $MnCl_2•4H_2O$, $FeCl_2•4H_2O$, $CoCl_2•2H_2O$, $NiCl_2•6H_2O$ and $CuCl_2•2H_2O$ with *L*-*α*-histidine in water have been determined by a microcalorimeter at 298.15—323.15 K. Fundamental parameters for the title reactions, the reaction rate constant (*k*), the apparent activation energy (*E*), the pre-exponential constant (*A*), the reaction order (*n*), the activation enthalpy ($\Delta H^{\neq}_{\ominus}$), the activation entropy ($\Delta S^{\neq}_{\ominus}$) and the activation free energy ($\Delta G^{\neq}_{\ominus}$) were calculated on the basis of thermodynamic and kinetic equations of the reactions.

The study revealed that, with the atomic number increasing, three thermodynamic parameters, $\Delta G^{\neq}_{\ominus}$, and $\Delta H^{\neq}_{\ominus}$, $\Delta S^{\neq}_{\ominus}$, present an analogy regularity.

References

1 Mohamed, E. H.; Antonino, P. M. *Anal. Biochem.* **1997**, *254*, 96.
2 Ji, M.; Liu, M.-Y.; Gao, S.-L.; Shi, Q.-Z. *Instrum. Sci. Technol.* **2001**, *29*, 53.
3 Kilday, M. V. *J. Research of NBS* **1980**, *85*, 467.
4 Nakamoto, K.; (Writer), Huang, D.-J.; Wang, R.-Q. (translator). *Infrared and Raman Spectra of Inorganic and Coordination Compounds*. 4th Edn, Chemical and Industrial Press, Beijing, **1991**, 253.
5 Donald, D. W.; Willian, H. E.; Vivian, B. P.; Pichard, H. S.; Iva, H.; Sylvia, M. B.; Kenneth, L. C.; Ralph, L. N. (writer), Liu, T.-H.; Zhao, M.-K. (translator). In *The NBS Table of Chemical Thermodynamic Properties*, Beijing, Chinese Standard Press, **1998**, pp. 2—198 (in Chinese).
6 Atkius, P. W. *Physical Chemistry*, 5th Edn., Oxford, Oxford University Press, C 9, **1997**.
7 Cox, J. D.; Harrop, D.; Head, A. *J. Chem. Thermodyn.* **1997**, *11*, 811.
8 Gao, S.-L.; Hou, Y.-D.; Ji, M. *Thermochim. Acta* **2000**, *351*, 47.
9 Gao, S.-L.; Chen, S.-P.; Hu, R.-Z. *Chin. J. Inorg. Chem.* **2002**, *18*, 362 (in Chinese).
10 Gao, S.-L.; Ji, M.; Chen, S.-P.; Hu, R.-Z.; Shi, Q.-Z. *J. Thermal. Anal. Calori.* **2001**, *66*, 423.

(E0403081 LI, W. H.)